Dynamics of Foaming of Polystyrene Particles

*Gabriela Salejova, Juraj Kosek**

September 24, 2006

Summary: In this work, we address the industrially relevant problem of the foaming of expandable polystyrene (PS) impregnated by pentane as a traditional down-stream processing in the suspension polymerization of styrene. Once the polystyrene foam is formed by means of a proper foaming agent, e.g., pentane or fluoro- or chlorohydrocarbons, the blowing agent diffuses out from the cellular structure. Environmental efforts call for the reduced consumption of blowing agents. The dynamics of foaming of polystyrene particles was recorded video-microscopically in our laboratory as the sequence of images of expanding particle located in the small pressure cell placed under the microscope with sufficient depth of focus. The amount of pentane sorbed in PS was controlled by the length of the impregnation period and was determined independently by gravimetric measurements. Strong dependence of the structure of the produced foam and of the foaming dynamics on the amount of sorbed pentane, temperature and particle size is reported and explanations for some observed foaming phenomena are provided.

Keywords: blowing agent; foaming; impregnation; Polystyrene; polystyrene foam; video-miscroscopy

Introduction

Thermoplastic foams represent an important class of materials that have advantageous cost and weight effective properties particularly in areas of impact strength, thermal and electrical insulation and lightweight structures. Polymeric foams can be produced by wide variety of processes ranging from expandable beads to injection moulding and extrusion.[1–2] The type of the foam and its final properties such as strength, density and insulating properties are determined by the type and concentration of the dissolved blowing agent, and by process parameters such as foaming temperature and pressure, cooling rate and the rate of pressure release or extrusion rate. The produced foam can be brittle, soft or resilient depending on the control of cell structure and induced orientation.

Although there is a considerable industrial expertise with foaming processes employing various grades of polymers, blowing agents and processing equipment, there is a need for improved process design when a change is required. One such change is necessitated by the phase-out of traditional blowing agents[3] due to environmental concerns. Chlorofluorocarbons (CFCs) were the original blowing agents of choice but were phased out due to concerns about their role in ozone depletion. Using CFCs it is relatively easy to produce foams with large number density and narrow size distribution of cells. Partially hydrogenated replacements of CFCs have been in use for several years as a temporary solution. Volatile organic compounds (VOCs) are sometimes used as physical blowing agents, but they are often flammable and/or tightly regulated. It can

Department of Chemical Engineering, Institute of Chemical Technology, Technicka 5, 166 28 Prague 6, Czech Republic
Phone: +420-220 44 3296; Fax: +420-220 44 4320
E-mail: Juraj.Kosek@vscht.cz

be challenging to maintain foam product quality while using more environmentally benign blowing agents such as N_2 or CO_2 which are inert but typically have a lower solubility in the polymer. Similar difficulties arise when a change in polymer, additives, or equipment is required.

Nucleating agents (e.g., talc powder) are often dispersed in the polymer matrix to provide heterogeneous nucleation sites and to control the number density and/or size distribution of cells in the final foam.[2] Comprehensive reviews of classical nucleation theory can be found elsewhere.[4–5] The cell structure of expanded foam is directly related to the number of bubbles nucleated during the foaming. Nucleation and growth affect the cell size distribution in synthetic polymer foaming, with nucleation having the strongest effect. The detailed discussion of the nucleation phase is available in Shen and Debenedetti,[6] Pai and Favelukis.[7] Good nucleating agents are expected to produce desirable foams with a large number density and narrow size distribution of bubbles.[8]

The foaming of thermoplastic polymers using physical blowing agents is a complex process. Many effects influence simultaneously the rheology of impregnated polymer and the microstructure of the product during the bubble growth. Theoretical analysis of bubble growth in polymer foams has been carried out by Shafi and Flumerfelt[9] and Koopmans et al.[10] Most of the previous work on polymer foaming is the theoretical study of bubble growth and only few experiments were reported that address the dynamic behavior of bubble growth in the molten polymer.[11–14] Other experimental studies have focused on the effect of polymer properties and operating conditions on the cellular structure of foams. The morphology of cellular structure is usually investigated experimentally after the foam has been formed.[15–17]

The microstructure of polymer foam, and the kinetics of the bubble growth within a pentane loaded molten PS sample is of relevance to the commercial foaming of polymers conducted by pressure release at the exit of an extruder. The foaming of expandable PS beads (impregnated by pentane) produced by the suspension process is also of industrial interest. The bubble growth data for polymeric foams are important for understanding the foam growth process and for testing the validity of models. Tuladhar and Mackley[18] carried out optical experiments using a Multipass Rheometer to follow the time evolution for melting the pentane loaded polystyrene beads. They were able to follow the growth kinetics of bubbles together with rheological measurements and formulated a model of the early stage of foaming including gas diffusion to fit the experimental data.

Here we report the results of videomicroscopy observations of polystyrene (PS) particles impregnated by pentane expanding during their foaming. We describe the initial foaming experiments and then discuss the effects of temperature, particle size and concentration of pentane in PS on the dynamics of foaming.

Experimental

Experimental equipment for the videomicroscopy observation of polystyrene particles expanding during their foaming consists of the observation cell equipped with two glass windows and of Nikon microscope with attached digital camera Nikon CoolPix 4500 (Figure 1). Two glass windows in the observation cell have a diameter 30 mm, thickness 8 mm and are kept in the distance 4 mm by the distance ring (Figure 2). The thickness of glass windows unavoidably causes some optical dispersion of images. The observation cell was designed as self-sealing so that high pressure forces both glass windows against O-rings placed in the metal part of the observation cell. It was found that the observation cell seals well also at vacuum conditions. The observation cell has an internal volume approx. 3 cm^3, is equipped with inlet and outlet capillaries, temperature and pressure probes and is thermo-

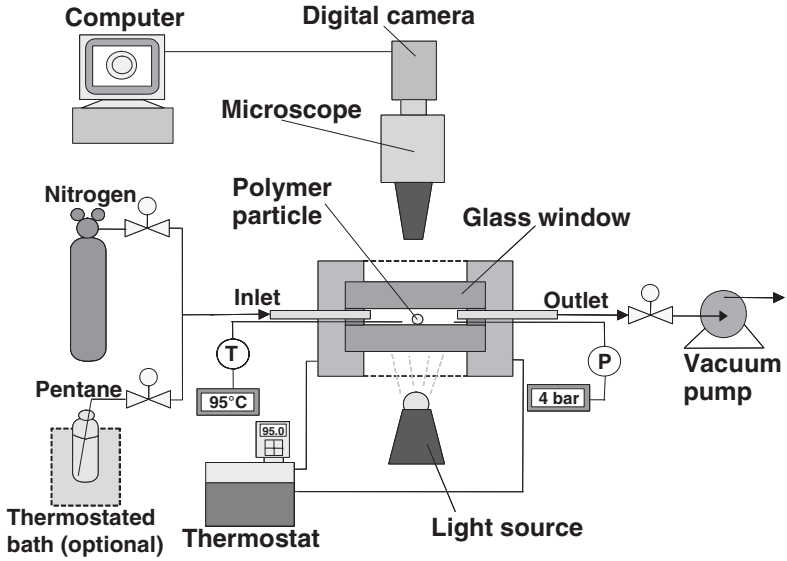

Figure 1.
Experimental apparatus for visual observation of particle foaming.

stated. Capillaries for the inlet and the outlet of gases/vapors and holes for temperature and pressure sensors cross the distance ring to the measuring space between the glass windows. The observed particles are placed into the observation chamber between the two glass windows and they are illuminated by a light source either from the top or from the bottom. The light applied from the bottom yields sharp contours of the particle, but the details of particle morphology are not visible. The illumination from top is employed in experiments reported in this paper because it was necessary to place the observed particle on the metal grid to prevent its lateral movements.

The observation vessel is heated by the circulation coil of the thermostat to the desired temperature. All inlet and outlet

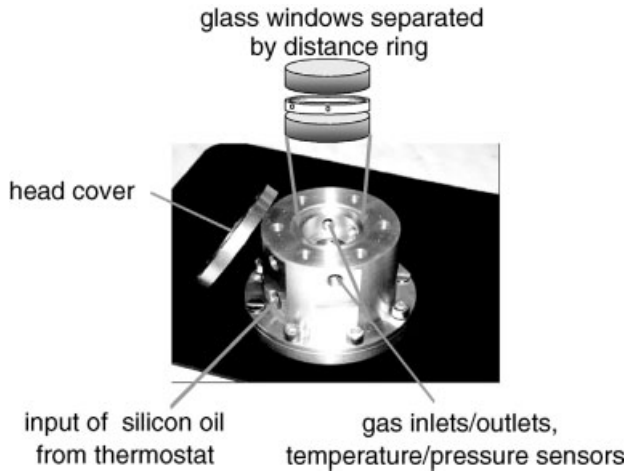

Figure 2.
The detail of the observation pressure cell.

capillaries and valves of the pressure cell are heated electrically by the resistance wire and their temperature is maintained by PID controller to prevent the condensation of pentane. The observation cell is partially thermally insulated from the environment and is protected from ambient light conditions by the cylindrical shield.

The digital camera is connected to the computer equipped with digital image-processing software LUCIA from Laboratory Imaging company. Changes in the area of particle image correspond to particle swelling or foaming. The first prototype of our experimental equipment was equipped with an analog camera attached to the microscope and the analog video signal was grabbed by the computer.

Experimental Procedure

Two different modes of particle foaming were carried out experimentally. Most experiments were run at constant temperature of the observation cell (between 85 °C and 105 °C). The particle of pure polystyrene was inserted into the observation cell, heated up to the required temperature and the observation cell was evacuated. Then the sorption of pentane in polystyrene particle(s) took place at specified pressure of pentane vapors for a predefined period of time t_{impreg} and finally the pressure was quickly released and the expansion of particle caused by the foaming was recorded. The advantage of this methodology is a well defined initial condition and starting time of the foaming. The dynamics of polystyrene impregnation by pentane was measured independently in our gravimetric apparatus.[19] The vapor pressure of pentane in the observation cell during the impregnation stage of measurement was controlled by a small pressure cylinder partially filled with liquid pentane and immersed into a thermostated bath with hot water. The pressure fluctuations during the charging of the observation cell by pentane lasted only several seconds and were weak so that they haven't caused the movement of the observed polystyrene particle.

The second mode of particle foaming was carried out at increasing temperature. The cold polystyrene particle impregnated by pentane was placed at a room temperature into the observation cell and the cell was hermetically sealed. The observation cell was then heated up and the particle foaming started suddenly at elevated temperature.

In both modes of foaming measurements the polystyrene particle was placed on the grid from the stainless steel coated by palladium black and located on the bottom glass in the observation cell. The grid prevented the particle movement, but the particle foaming was not restricted by the grid. The observation cell was hermetically closed by the upper flange and the whole equipment was put under the microscope lens. The pressure-leak test of the apparatus was done by nitrogen. Setting of video-microscopy equipment was adjusted to have the sharp image of the observed particle.

After the temperature has stabilized at the predefined constant value, the vacuum was applied and the unchanging size of particle was verified by the digital processing of several images captured during 10 min. The high depth of focus was achieved by means of the optic adaptor mounted between the microscope and the digital camera with the variable length of focus. Thus a low magnification (and therefore high depth of focus) was set at the microscope and the magnification was enhanced by the optical zoom of the digital camera. The setting of the microscope, i.e., its focusing, magnification and intensity of illumination was kept constant during the experiments. Figure 3 shows an example of the digital image of the particle during its foaming.

During the measurements, the automatic scanning of images was set in regular time intervals of 10 s. The sequences of images of polystyrene particles were processed by the LUCIA software in several steps. First, the contrast of the image was adjusted to the level suitable for the image binarization and a threshold function for

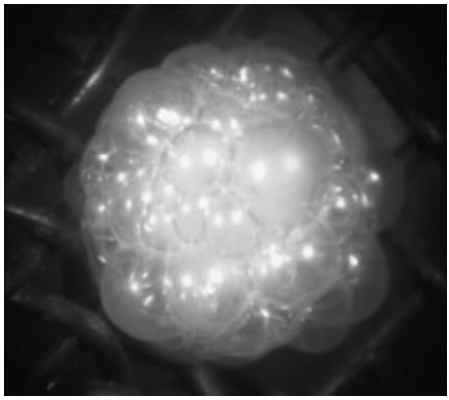

Figure 3.
The image of expanding polystyrene particle taken in the observation cell by the digital camera.

the binarization of the image was determined. This threshold function analyses the colors of the image and distinguishes the particle from the background. In the case of sufficient contrast, the results of image processing are almost independent of image binarization parameters. We haven't employed the possibility of the calibration of the actual length scale because we were interested only in relative changes of particle area during its foaming.

After the binarization the software LUCIA evaluates a particle size and reports it as the equivalent diameter of the perfect sphere with the same area like the observed (non-spherical) particle. This method is automatically repeated for the recorded sequence of images and the evolution of the particle equivalent diameter is obtained both for the sorption of pentane and for the foaming. The change of particle volume can be simply characterized with the third power of the equivalent particle diameter.

The experimental apparatus for video-microscopy observation of particle foaming has been continuously improved during the measurements. The most important changes were the installation of digital camera and associated increase of the depth of focus and the stabilization of the illumination.

Results and Discussion

The polystyrene powder with a trade name Koplen provided by KAUČUK company was pre-sieved into fractions. The fractions with particle size 0.63 to 0.90 mm and 0.90 to 1.25 mm were chosen for foaming experiments, but some experiments were conducted with smaller or larger particles. n-pentane of purity 97% was employed as a blowing agent for impregnation of PS particles. The primary objective of our measurements was to determine the dependence of foaming dynamics of a single PS particle on: (i) the amount of pentane sorbed in particle, (ii) on the temperature, and (iii) on the particle size. In our measurements the amount of pentane sorbed in PS particle depends on the period of impregnation t_{impreg} and on the conditions of impregnation. The foaming is described quantitatively by the foaming ratio (V/V_0) defined as the ratio of the actual particle volume V and the volume of the compact particle before the foaming V_0.

Initial Foaming Experiments

In the initial series of constant-temperature experiments, the impregnation of PS particle(s) by pentane was not carried out at a constant pressure of pentane. The observation cell was charged by pentane only at the start of impregnation and the pressure was freely decreasing as the pentane sorbed into the particle. After the impregnation period t_{impreg}, the pressure cell was evacuated and the particle has expanded on the time scale of several minutes as a consequence of its foaming. After several minutes the particle size has reached its maximum and then it slightly decreased in some experiments.

The first successful foaming experiment with the PS particle of approx. 1 mm diameter impregnated for $t_{\mathrm{impreg}} = 63.6$ min at 95 °C by pentane with the initial pressure $p_0 = 4.2$ bar is displayed in Figure 4. The pressure of pentane has decreased during the impregnation from 4.2 bar to 3.38 bar as a result of sorption. The foaming ratio in

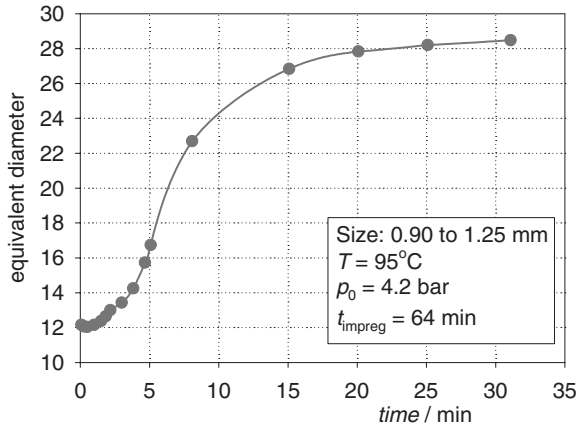

Figure 4.
Foaming of PS particle impregnated with pentane into vacuum at $T = 95\,^{\circ}C$. Impregnation of PS particle with diameter approx. 1 mm was done by pentane with initial pressure $p_0 = 4.2$ bar at 95 °C for $t_{impreg} = 63.6$ min.

this experiments was $(V/V_0) = (28.5/12.0)^3 = 13.4$ which is a number smaller than a typical foaming ratio in industry. Let us note that a significant expansion of the particle started with a certain delay after the sudden application of the vacuum in the observation cell. The time on the horizontal axis of Figure 4 starts by the application of vacuum.

The growth of individual bubbles (cells) was also observed. The images representing the evolution of the particle structure during the foaming are shown in Figure 5. The quality of images in Figure 5 is limited by the depth of the focus of the microscope with attached analog camera. Nevertheless we can observe the formation and growth of relatively large bubbles.

We were not able to estimate the swelling of PS particles by pentane, i.e., the dependence of particle diameter on impregnation time, due to the large uncertainty of digital image processing of results of these measurements. PS particles have changed their color from white to gray during the impregnation by pentane so that the contrast between the particle and the background has diminished and it was thus not possible to obtain sharp and unambiguous contours of particles in the binarization step of digital image processing.

Figure 6 shows the dynamics of pentane sorption into PS powder at 95 °C and pentane pressure 4 bar, i.e., at conditions employed typically in our video-microscopy measurements of foaming. This Figure relates the impregnation period and the amount of pentane sorbed in PS. For example, impregnation time $t_{impreg} = 60$ min at 95 °C and pentane pressure 4 bar results in 8.0 wt.% of pentane in PS. However, the radial concentration profile of pentane in individual particles is not uniform. We performed number of systematic measurements of both concentration and temperature dependent transport of pentane in PS and of equilibrium sorptions of pentane in PS in the temperature range from 45 to 120 °C. However results of these measurements do not fit to the limited size of this paper.

Effect of Impregnation Time on Particle Foaming

The effect of impregnation time on the foaming of PS particles has been investigated in a systematic series of measurements. The particles were impregnated by pentane at constant pressure $p = 4.0$ bar and temperature 95 °C for a period $t_{impreg} = 10$,

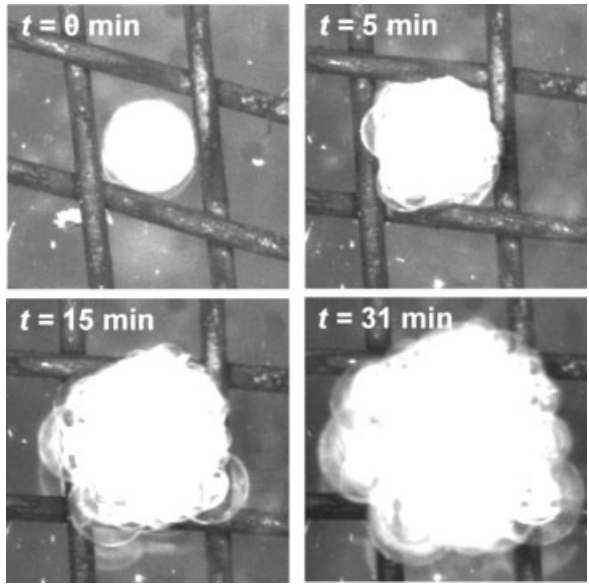

Figure 5.
The sequence of images for experiment described in Figure 4. Foaming started by application of vacuum after the impregnation of PS by pentane for a period $t_{impreg} = 63.6$ min.

20, 30 or 60 min. In this series of experiments the pressure of pentane was maintained at constant level by thermostating the cylinder containing liquid pentane and keeping it connected with the observation cell. The amount of sorbed pentane can be estimated from the sorption dynamics determined by gravimetric measurements, cf. Figure 6, but the characteristic size of particles has to be taken into account.

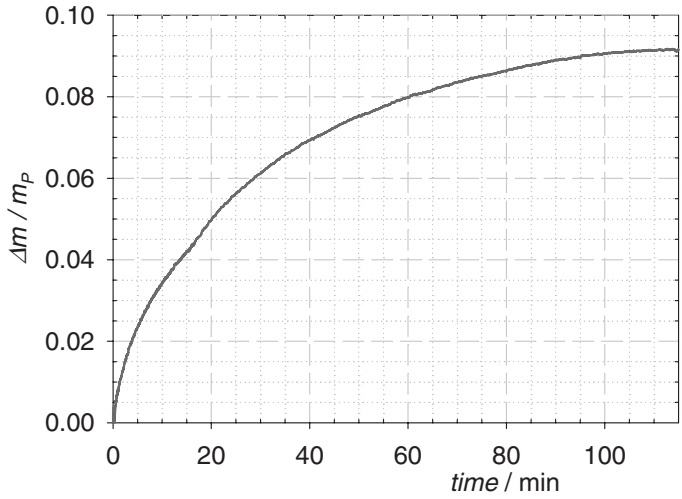

Figure 6.
Dynamics of pentane sorption in approx. 1 g of PS powder (fraction of particle size 0.90 to 1.25 mm) at 95 °C and constant pressure of pentane 4 bar determined gravimetrically. Vertical axis is the ratio of the mass of sorbed pentane Δm to the mass of pure polymer m_P.

The comparison of the dynamics of foaming for the considered cases is summarized in Figure 7, which displays the time evolution of the foaming ratio (V/V_0). The pentane was suddenly evacuated at time $t = 0$ s and the foaming has started at this time. The intensive growth of cells has appeared approximately 30 s after the evacuation of the observation cell. The expansion of PS particles was nearly complete at $t = 200$ s regardless the impregnation time preceding the foaming. The foaming ratio (V/V_0) increases with increasing impregnation time of PS particles by pentane.

The amount of pentane sorbed in PS particle influences also the morphology of the arisen foam, cf. Figure 8. The evolution of the foam structure in this Figure depends on the impregnation period t_{impreg} preceding the application of vacuum. The cellular structure of the expanded particle is homogeneous for a short impregnation period and individual cells in the foam are relatively small. On the other hand, at long impregnation periods the final cellular structure of the expanded particle is heterogeneous and large semi-transparent bubbles randomly arise close to the particle surface.

A similar series of experiments investigating the effect of impregnation period on foaming was performed at 95 °C with the older experimental setup where the observation cell was charged by pentane with initial pressure p_0 and then the pentane pressure was slowly decreasing because of pentane sorption in PS and because of the small volume of the observation cell. After 60 min of impregnation the pressure of pentane vapors has decreased about 0.5 bar. Vacuum conditions were again applied during the foaming of impregnated PS particles, cf. Figure 9.

In Figure 9 we observe that the foaming is counter-intuitively faster and the particle foaming ratio (V/V_0) higher during the shorter impregnation time of pentane $t_{\mathrm{impreg}} = 30$ or 60 min than during the long impregnation time $t_{\mathrm{impreg}} = 90$ min. Explanation of this observation shall take into consideration: (i) amount of pentane and concentration profile of pentane in the particle, (ii) concentration- and temperature-dependent rate of pentane diffusion in polymer and out of particle, (iii) cooling of particle as a consequence of phase separation of pentane from PS, (iv) temperature and concentration-dependent visco-elastic properties of PS impregnated by pentane, and (v) rate and density of formation of nucleation centers.

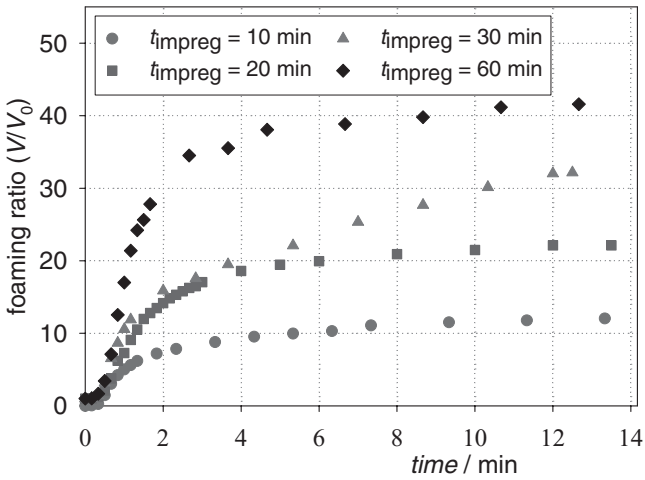

Figure 7.
Foaming dynamics of polystyrene particle (taken from size fraction 0.63 to 0.90 mm) impregnated by pentane at temperature 95 °C and pressure 4.0 bar for time t_{impreg}. Foaming was carried out at 95 °C and at vacuum conditions.

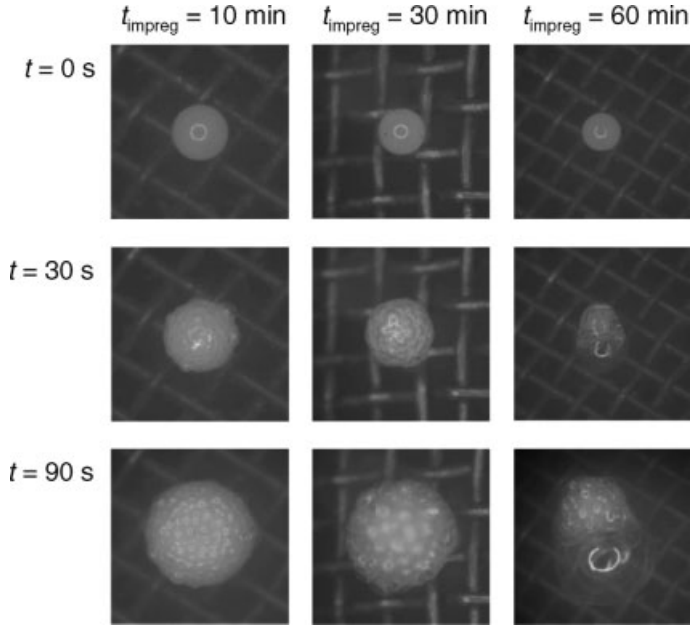

Figure 8.
The formation of the foam structure during the expansion after various periods of impregnation. The conditions of impregnation and foaming are described in Figure 7. Each vertical column of images corresponds to a slightly different setting of a microscope.

The foaming ratio (V/V_0) in Figure 9 is similar for $t_{impreg} = 30$ min and $t_{impreg} = 60$ min because the initial pressure of pentane p_0 at 60 min was smaller. Our working hypothesis explaining the different dynamics of foaming with a long induction period for $t_{impreg} = 90$ min is the strong concentration dependence of pentane transport in PS and visco-elastic properties of PS impregnated by pentane. As we show

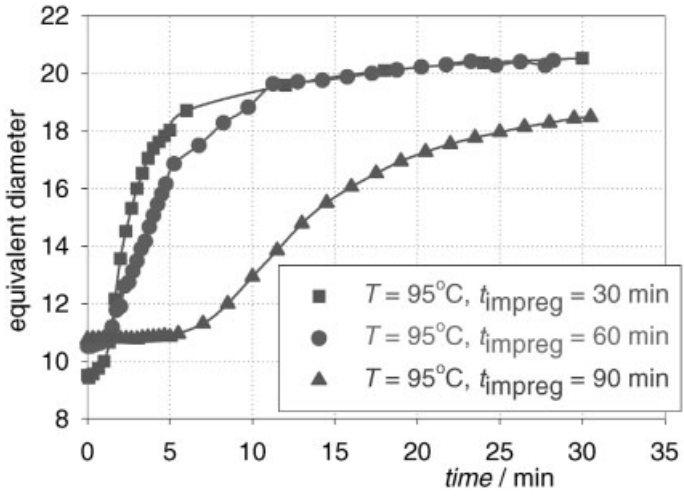

Figure 9.
Foaming of PS particle (taken from size fraction 0.90 to 1.25 mm) impregnated with pentane into vacuum at temperature 95 °C. PS particle was impregnated at 95 °C by pentane with initial pressure $p_o = 4.1$ bar for period $t_{impreg} = 30$ min, $p_o = 3.8$ bar for $t_{impreg} = 60$ min, and $p_o = 3.5$ bar for $t_{impreg} = 90$ min.

below, the higher fraction of pentane sorbed in PS does not necessarily translate into larger foaming ratio (V/V_0) and is sometimes associated with a longer induction period of foaming similarly as in the case shown in Figure 9. Relatively small initial pressure of pentane $p_0 = 3.5$ bar for $t_{impreg} = 90$ min might also contribute to counter-intuitive behavior displayed in Figure 9.

Effect of Temperature on Particle Foaming

The effect of temperature on the foaming of polystyrene particles has been investigated at temperatures 85, 90, 95, 100 and 105 °C and is summarized in Figure 10. The impregnation of particles by pentane lasted $t_{impreg} = 60$ min and was done at the same temperature as the subsequent foaming. The attempts to foam the impregnated particle at 85 °C by the sudden release of pressure were not successful or were not reproducible. The rate of foaming slows down and the foaming ratio (V/V_0) decreases with the increasing temperature, cf. Figure 10 and Table 1. Figure 10a compares two almost identical foaming experiments carried out at 90 °C. The rate of foaming has been the same in both experiments but the foaming ratio was different because of the initial pressure of pentane p_0 set at the start of the impregnation stage. Some variability of experimental results is also caused by small differences in diameters of employed polystyrene particles.

Foaming ratios (V/V_0) are summarized in Table 1 and were calculated as the ratio of

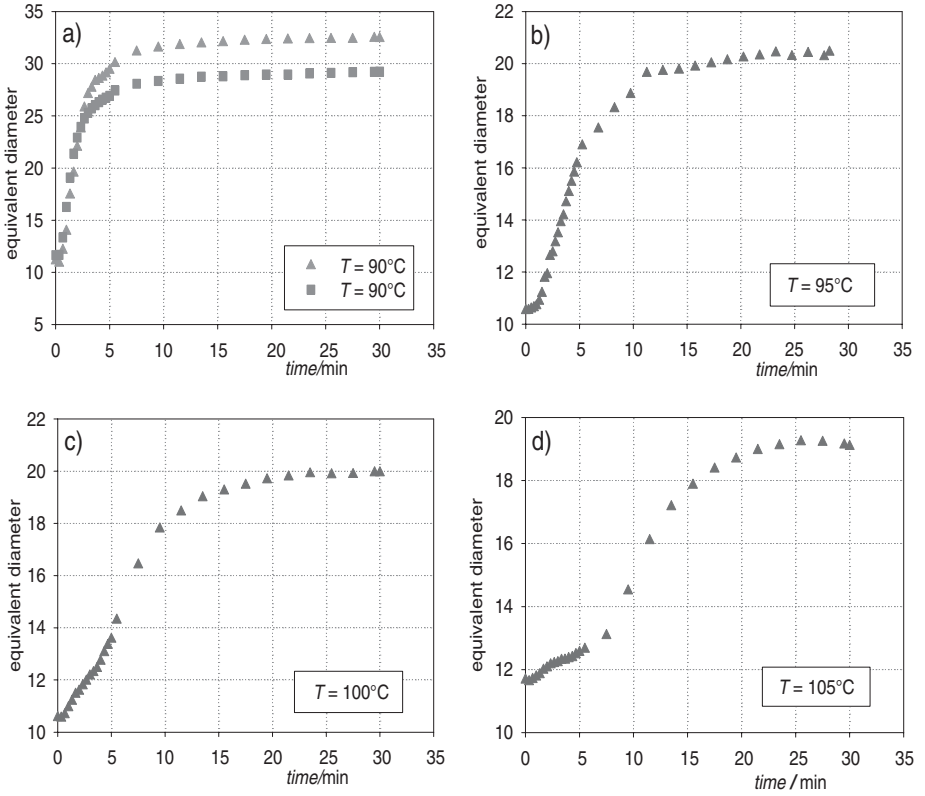

Figure 10.
Foaming of PS particles impregnated by pentane for a period of 60 min in dependence on temperature: **a)** 90 °C (two experiments), **b)** 95 °C, **c)** 100 °C, **d)** 105 °C. Detailed conditions of experiments are listed in Table 1.

Table 1.
Conditions of impregnation/foaming experiments investigating the effect of temperature.

Temperature	Size fraction of PS particle	Pentane pressure in impregnation p_o	Impregnation period t_{impreg}	Foaming ratio (V/V_o)
90 °C	0.90 to 1.25 mm	3.6 bar	60 min	$(29.2/11.7)^3 = 15.6$
90 °C	0.90 to 1.25 mm	4.0 bar	60 min	$(32.4/11.1)^3 = 24.9$
95 °C	0.90 to 1.25 mm	3.8 bar	60 min	$(20.3/10.4)^3 = 7.4$
100 °C	0.90 to 1.25 mm	4.0 bar	60 min	$(19.9/10.5)^3 = 6.8$
105 °C	0.90 to 1.25 mm	3.0 bar	60 min	$(19.1/11.6)^3 = 4.5$

third powers of evaluated equivalent diameters of particles (in arbitrary units). For example, in the case of the second experiment listed in Table 1 the particle equivalent diameter has expanded almost three times which roughly corresponds to industrially relevant requirements on foaming.

At 90 °C the PS particle expands immediately after the application of vacuum and most of volume expansion is over after 5 min of foaming, cf. Figure 10a. At higher temperatures (especially at 100 °C and 105 °C) we observe the delay in foaming, i.e., the presence of an induction period of slow particle expansion after the application of vacuum, cf. Figure 10c,d. The foaming dynamics for the first experiment from Table 1 is shown in Figure 11. A gray color of PS particle impregnated by pentane can be observed. The best results with foaming ratio $(V/V_0) = 25$ were achieved at temperature 90 °C maintained both during the impregnation and foaming stage of the experiment. The foaming dynamics at temperatures higher than 90 °C became worse with the size of particles used in this study.

The explanation of foaming profiles in Figure 10 has to take into consideration not only temperature, but also faster diffusion of pentane out of the impregnated PS particle at higher temperature and larger fraction of pentane in PS particles impregnated at higher temperatures. We suggest that at higher temperatures the individual cells expand but a significant fraction of pentane diffuses out of the particle and the polymer impregnated by pentane is soft to

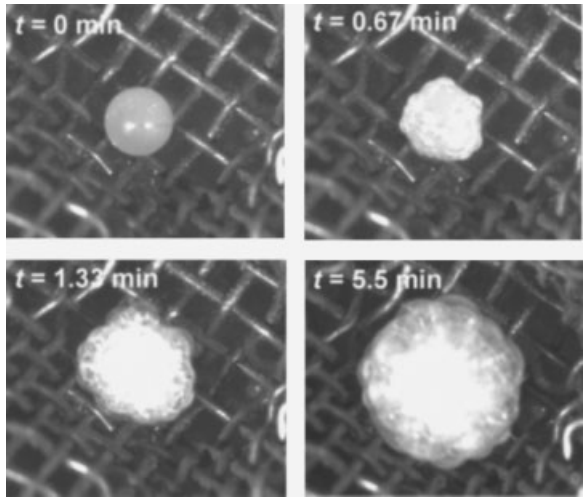

Figure 11.
The sequence of images taken during the foaming of PS particle (size fraction 0.90 to 1.25 mm) impregnated for 60 min by pentane with initial pressure $p_o = 3.6$ bar at 90 °C and then subjected to vacuum at the same temperature.

Table 2.
Conditions of impregnation/foaming experiments investigating the effect of particle size.

Temperature	Size fraction of PS particle	Pentane pressure in impregnation p	Impregnation period t_{impreg}	Foaming ratio (V/V_0)
95 °C	0.40 to 0.63 mm	4.2 bar	30 min	$(1.45/0.53)^3 = 20.4$
95 °C	0.63 to 0.90 mm	4.1 bar	30 min	$(2.73/0.78)^3 = 42.4$
95 °C	0.63 to 0.90 mm	4.1 bar	30 min	$(2.76/0.79)^3 = 41.9$
95 °C	0.90 to 1.25 mm	4.2 bar	30 min	$(4.13/1.12)^3 = 50.9$
95 °C	1.25 to 1.60 mm	4.2 bar	30 min	$(5.71/1.44)^3 = 61.9$
95 °C	1.60 to 2.50 mm	4.0 bar	30 min	$(8.71/2.17)^3 = 64.9$
95 °C	1.60 to 2.50 mm	4.0 bar	30 min	$(7.34/2.10)^3 = 42.6$

hold the bubbles permanently. Therefore the optimum temperature and other conditions for particle foaming are conditions where the expanded cellular structure will quickly become ''frozen'. The presence of the induction period in the foaming profile does not depend only on temperature but also on the initial pressure of pentane p_0 set at the start of the impregnation period.

Effect of Particle Size on Foaming

The effect of particle size on dynamics of particle foaming was investigated in another series of experiments. The size of particles affects both the space-averaged concentration of pentane in the particle and the concentration profile of pentane in the particle. The content of pentane in PS thus depends both on the impregnation time and on the particle size. The experimental procedure for the impregnation of PS particle by pentane and subsequent foaming by subjecting the particle to vacuum remained the same. Both impregnation and foaming were carried out at the same temperature. The pressure of pentane was kept constant at approx. 4 bar during the impregnation, cf. Table 2.

The summary of foaming experiments with particles of different diameters impregnated for a period of 30 min by pentane at temperature 95 °C and pressure approx. 4 bar is given in Figure 12. We have intentionally used the impregnation period $t_{impreg} = 30$ min because we supposed that this relatively short impregnation time will affect the foaming of large particles. However, we were surprised to observe

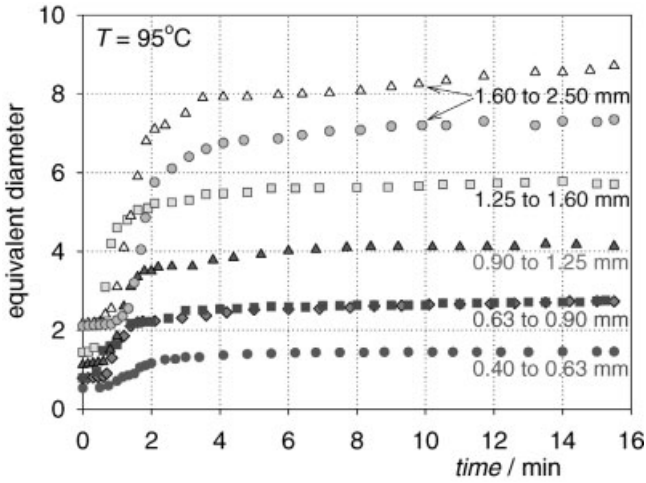

Figure 12.
Foaming of PS particles impregnated by pentane in dependence on particle size (size fractions of particles are given). PS particles were impregnated by pentane for period $t_{impreg} = 30$ min at 95 °C and then subjected to vacuum at the same temperature. Detailed conditions of experiments are listed in Table 2.

that the foaming ratio (V/V_0) has increased for larger particles. The variability of the foaming ratio (V/V_0) at last two rows of Table 2 is caused by the uncertainty in the binarization step of image processing, i.e., in the automatic identification of the boundary of the foamed particle.

The dependence of foaming ratio (V/V_0) on particle diameter again points out on the importance of pentane transport in PS during the foaming. Larger particles have smaller surface-to-volume ratio and hence the diffusion flux of pentane into surrounding vacuum scaled per the unit volume of particle is smaller. Large particles are thus losing relatively small amount of pentane by the diffusion to the surrounding vacuum and hence more pentane is involved in the formation and growth of individual cells.

Foaming of Impregnated PS Particles at Increasing Temperature

We use the term foaming at increasing temperature for experiments where the cold PS particle already impregnated by pentane was heated in the observation cell and started to expand during its heating. A typical experiment with the PS particle originally containing 7.2 wt.% of the ''frozen'' pentane is shown in Figure 13.

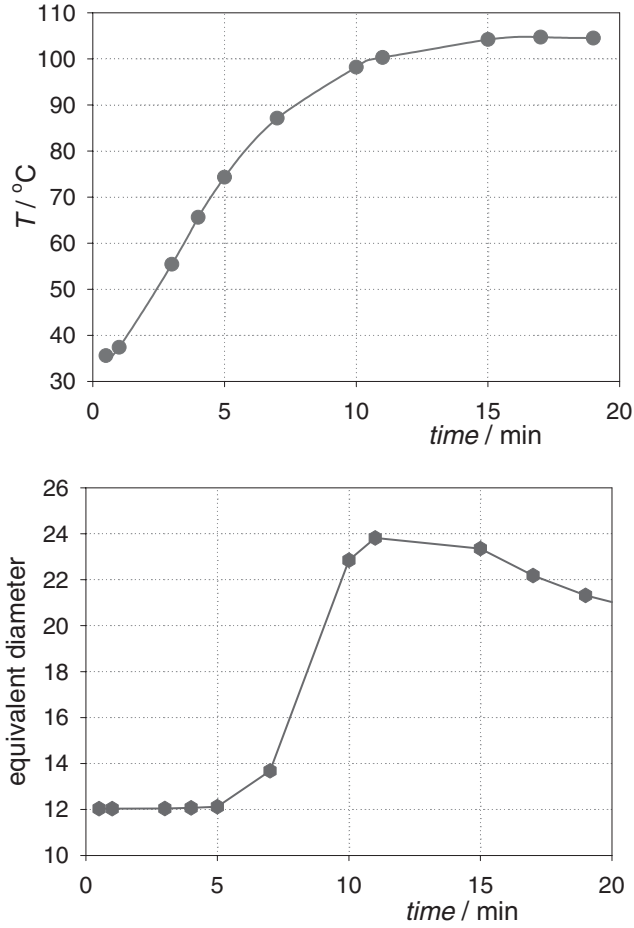

Figure 13.
Foaming of PS particle (size fraction 0.90 to 1.25 mm) impregnated originally with 7.2 wt.% of pentane at increasing temperature.

Vacuum conditions were not applied during the experiment and the pressure was allowed to freely develop in the hermetically closed observation cell. The final pressure measured in the sorption cell at 105 °C was 1.74 bar. We can observe the dramatic expansion of particle at temperature between 80 and 90 °C and subsequently the expanded particle slightly shrinks. The shrinking can be caused by the partial collapse of cells of the softened polymer impregnated by pentane, or by the deformation of the cellular structure by the external pressure.

In reality all our foaming experiments, even those run at a constant temperature of the observation cell, were non-isothermal with respect to the expanding particle. Pentane desorbing from the particle into the gas phase consumes the heat required for its phase transfer from the polymer-solvent mixture into the vapor phase. The expanding particle is thus cooled down during its foaming.

Conclusions

The dynamics of foaming of individual polystyrene beads was investigated in the pressure observation cell and was recorded by video-microscopy. The effects of the impregnation time (related to concentration of pentane in polystyrene), temperature and particle size were examined. The main difference from typical manufacturing conditions employed in the foaming of PS beads was the absence of steam used for heating of expandable beads. In our experiments the foaming was conducted at vacuum conditions because the presence of steam partially condensing on glass windows in the observation cell would impair the quality of images.

We have demonstrated the importance of pentane transport in PS both during the impregnation and during the foaming on the quality of the resulting cellular structure, on the dynamics of foaming and on the foaming ratio (V/V_0) defined as the ratio of the actual particle volume V and the volume of the compact particle before the foaming V_0. For certain conditions (e.g., at higher temperature) the foaming does not start immediately after subjecting the impregnated particle to vacuum, but after some delay. The cellular structure of the expanded particle is homogeneous and individual cells are small in the case of a short impregnation time.

Acknowledgements: The support from the Czech Grant Agency (project 104/03/H141) and from the Ministry of Education (MSM 6046137306) is acknowledged.

[1] K. Joshi, J. G. Lee, M. A. Sha, R. W. Flumerfelt, *Journal of Applied Polymer Science* **1998**, *67*, 1353.
[2] S. T. Lee, "*Foam extrusion: principles and practice*", Technomic, Lancaster, PA 2001.
[3] J. Sharpe, D. MacArthur, M. Liu, T. Kollie, R. Graves, R. Hendriks, *Journal of Cellular Plastics* **1995**, *31*, 313.
[4] M. Blander, J. L. Katz, *AIChE Journal* **1975**, *21*, 833.
[5] A. Laaksonen, V. Talanquer, D. W. Oxtoby, *Annual Review of Physical Chemistry* **1995**, *46*, 489.
[6] V. K. Shen, P. G. Debenedetti, *Journal of Chemical Physics* **2003**, *118*, 768.
[7] V. Pai, M. Favelukis, *Journal of Cellular Plastics* **2002**, *38*, 403.
[8] R. McClurg, *Chemical Engineering Science* **2004**, *59*, 5779.
[9] M. A. Shafi, R. W. Flumerfelt, *Chemical Engineering Science* **1997**, *52*, 627.
[10] R. J. Koopmans, J. C. F. den Doelder, A. N. Paquet, *Advanced Materials* **2000**, *12*, 1873.
[11] C. A. Villamizar, C. D. Han, *Polymer Engineering and Science* **1978**, *18*, 687.
[12] C. A. Villamizar, C. D. Han, *Polymer Engineering and Science* **1978**, *18*, 699.
[13] N. S. Ramesh, D. H. Rasmussen, G. A. Campbell, *Polymer Engineering and Science* **1991**, *31*, 1657.
[14] K. Taki, T. Yatsuzuka, M. Ohshima, *Journal of Cellular Plastics* **2003**, *39*, 155.
[15] N. S. Ramesh, D. H. Rasmussen, G. A. Campbell, *Polymer Engineering and Science* **1994**, *34*, 1697.
[16] J. Pallay, P. Kelemen, H. Berghmans, D. V. Dommelen, *Macromolecular Materials and Engineering* **2000**, *275*, 18–25.
[17] A. Elmoutaouakkil, G. Fuchs, P. Bergounhon, R. Peres, F. Peryin, *Journal of Physics D: Applied Physics* **2003**, *36*, p. A37.
[18] T. R. Tuladhar, M. R. Mackley, *Chemical Engineering Science* **2004**, *59*, 5997.
[19] A. Novak, M. Bobak, J. Kosek, B. J. Banaszak, D. Lo, T. Widya, W. H. Ray, J. J. de Pablo, *Journal of Applied Polymer Science* **2006**, *100*, 1124.

